Wurtzite-derived polytypes of kesterite and stannite quaternary chalcogenide semiconductors

Shiyou Chen,[1,2] Aron Walsh,[1,3] Ye Luo,[1] Ji-Hui Yang,[1] X. G. Gong,[1] and Su-Huai Wei[4]
[1]*Laboratory for Computational Physical Sciences and Surface Physics Laboratory, Fudan University, Shanghai 200433, China*
[2]*Laboratory of Polar Materials and Devices, East China Normal University, Shanghai 200241, China*
[3]*Department of Chemistry, University College London, London WC1E 6BT, United Kingdom*
[4]*National Renewable Energy Laboratory, Golden, Colorado 80401, USA*
(Received 20 September 2010; published 15 November 2010)

The I_2-II-IV-VI_4 quaternary chalcogenide semiconductors (e.g., Cu_2ZnGeS_4, Cu_2ZnSnS_4, $Cu_2ZnGeSe_4$ $Cu_2CdSnSe_4$, and $Ag_2CdGeSe_4$) have been studied for more than 40 years but the nature of their crystal structures has proved contentious. Literature reports exist for the stannite and kesterite mineral structures, which are zinc-blende-derived structures, and wurtzite-stannite, which is a wurtzite-derived structure. In this paper, through a global search based on the valence octet rule (local charge neutrality), we report a wurtzite-derived structure corresponding to the kesterite structure, namely, wurtzite-kesterite (space group *Pc*), which is the ground state for some I_2-II-IV-VI_4 compounds, but is easily confused with the wurtzite-stannite (space-group $Pmn2_1$) structure. We show that there is a clear relationship between the properties of the wurtzite-kesterite and zinc-blende-derived kesterite structures, as well as between wurtzite-stannite and stannite. Contributions from the strain and Coulomb energies are found to play an important role in determining the structural stability. The underlying trends can be explained according to the size and ionicity of the group-I, -II, -IV, and -VI atoms. Electronic-structure calculations show that the wurtzite-derived structures have properties similar to the zinc-blende-derived structures, but their band gaps are relatively larger, which has also been observed for binary II-VI semiconductors.

DOI: 10.1103/PhysRevB.82.195203 PACS number(s): 61.50.Ah, 71.20.Nr, 71.22.+i, 71.70.Fk

I. INTRODUCTION

The I_2-II-IV-VI_4 (I=Cu,Ag; II=Zn,Cd; IV=Si,Ge,Sn; VI=S,Se) series of quaternary chalcogenide semiconductors have drawn wide interest for their potential application as solar-cell absorbers,[1–9] photocatalysts for solar water splitting,[10] thermoelectric materials,[11–14] and even for their magneto-optic and multiferroic properties when alloyed with Mn.[15–17] For example, Cu_2ZnSnS_4 (CZTS) and $Cu_2ZnSnSe_4$ (CZTSe) are naturally abundant and environmentally friendly thin-film solar-cell absorbers, which have shown conversion efficiencies as high as 10%.[1,9]

The wide application of these quaternary compounds comes from their increased chemical and structural freedom, which makes their physical properties more flexible relative to binary and ternary compounds.[12,18] However, the increased freedom also makes the study of these quaternary compounds more complicated, e.g., characterization of their crystal structures. Although Rietveld refinement using conventional x-ray diffraction patterns gives the space-group character, the occupation of different atomic sites by group-I, -II, and -IV cations cannot be determined accurately for two reasons: (i) the cations that are close in the periodic table have similar x-ray scattering factors, thus ordering for Cu-Zn, Zn-Ge, Ag-Sn, and Cd-Sn is difficult to determine;[19] (ii) the sample quality of these quaternary semiconductors is usually poor. The number of possible configurations is large, and it is difficult to consider all the configurations exhaustively in fitting the x-ray diffraction pattern.

In the literature, it has been generally assumed that I_2-II-IV-VI_4 compounds adopt one of two structures: stannite [Fig. 1(d)] and wurtzite-stannite [Fig. 1(c)], as reviewed in the Landolt-Börnstein handbook.[20] Recent experimental and theoretical studies have revealed that Cu_2ZnSnS_4 and $Cu_2ZnSnSe_4$ crystallize in the kesterite structure [Fig. 1(b)] as their ground-state structure but kesterite may be confused with stannite due to occupational disorder of the Cu and Zn cations.[21–23] In our previous study, we have shown that the I_2-II-IV-VI_4 stannite (ST) and kesterite (KS) structures can be derived through a two-step cation substitution in the binary II-VI zinc-blende (ZB) structure.[18] For example, by substituting two Zn in ZB ZnS (II-VI) by Cu+Ga we obtain $CuGaS_2$, a I-III-VI_2-type ternary semiconductor, and there are two possible structure configurations with the smallest

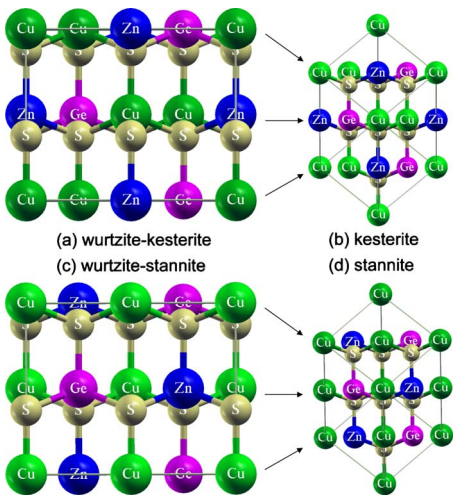

FIG. 1. (Color online) Crystal-structure representations of (a) wurtzite-kesterite, (b) kesterite, (c) wurtzite-stannite, and (d) stannite. The arrows show the corresponding relation between the (0001) planes of the wurtzite-derived structure and (111) planes of the zinc-blende-derived structure.

 ©2010 The American Physical Society

eight-atom cell, i.e., (201) cation ordering in chalcopyrite (CH) and (001) ordering in CuAu-like (CA) structures. Further replacement of two Ga ions in the $CuGaS_2$ CH structure by Zn+Sn results in the Cu_2ZnSnS_4 KS structure. Similarly, mutation of the CA structure results in ST. In this substitution, the valence octet rule,[24,25] which states that the configurations with all anions in an eight-electron closed-shell state (local charge neutrality) have lower energy, is assumed. Indeed, both the KS and ST structures obey the valence octet rule and are found as the lowest-energy ZB-derived structures according to first-principles total-energy calculations.

Binary semiconductors with ionic character such as CdS crystallize in the wurtzite (WZ) structure as their ground state, due to the favorable Madelung energy of the hexagonal close-packed WZ lattice relative to the face-centered-cubic ZB structure. For ternary I-III-VI_2 compounds (III=Ga,In), reports of the WZ-derived polytypes have been scarce, with known examples including $CuInS_2$ nanodisks.[26,27] Among quaternary I_2-II-IV-VI_4 semiconductors, WZ-derived structures have been reported and are usually called orthorhombic structures for Cu_2ZnGeS_4, $Cu_2ZnGeSe_4$, Cu_2CdGeS_4, $Ag_2CdSnSe_4$, etc.,[10,20,28,29] but the relative stability of the ZB- and WZ-derived structures has never been studied. Furthermore, literature reports have been restricted to the wurtzite-stannite structure and it is not clear if there are other low-energy WZ-derived structures for quaternary chalcogenides. As more attention is being paid to the application of these materials, it becomes necessary to have a complete and clear understanding of different structure configurations and their influence on the electronic and other physical properties.

In this paper, we report results from a global search for the atomic configurations of the quaternary WZ-derived structures that obey the octet rule. We report two fundamental structures with 16-atom primitive unit cells: the wurtzite-kesterite and wurtzite-stannite structures, which correspond to the ZB-derived kesterite and stannite structures, respectively. The former structure has not been reported in the literature for chalcogenides and is the ground-state structure for some I_2-II-IV-VI_4 compounds but may be confused with the wurtzite-stannite structure in diffraction experiments. First-principles total-energy calculations show that the energy stability between the ZB- and WZ-derived structures exhibits a clear dependence on the cation size difference and the ionicity of I_2-II-IV-VI_4 compounds. Electronic-structure analysis shows that the band component has similar character for the ZB- and WZ-derived structures, despite that the band gaps of the WZ-derived compounds are slightly larger than the ZB-derived structures, consistent with the trend for binary II-VI compounds.

II. STRUCTURE CONFIGURATIONS

As we have highlighted, cation ordering in the quaternary systems can be difficult to assess experimentally, thus it is important to search theoretically for possible structural configurations with low energy. Since it has been well demonstrated that the octet rule plays an important role in the energy stability of different I_2-II-IV-VI_4 structural configurations,[18,22] we can use this as an initial energy descriptor and screen the high-energy structure configurations that violate this rule. Due to the low cost of evaluating the energy, complete enumeration of all ZB- and WZ-derived cation ordering combinations was performed. Additionally, a genetic algorithm was implemented based on the octet rule, which arrived at the ground-state configuration more rapidly.[30] Two ZB-derived (eight-atom primitive cells) and two WZ-derived (16-atom primitive cells) configurations emerged from our search (Fig. 1). There are further configurations with larger unit cells that obey the octet rule, but we will focus on those with the smallest primitive cells since they are expected to be representative of the properties for the larger cells.[31]

The two WZ-derived structures we find include: (i) the wurtzite-stannite structure [Fig. 1(c), space-group $Pmn2_1$], which has been observed as the high-temperature phase of Cu_2ZnGeS_4 above 810 °C,[28] and the magnetic semiconductors Cu_2MnGeS_4 and Ag_2MnSiS_4.[32] (ii) A new structure [Fig. 1(a), space-group Pc], which has not been reported for these chalcogenide semiconductors, although a similar structure has been reported for quaternary oxide materials including Li_2ZnGeO_4.[33,34]

In Table I, the crystallographic parameters of the two WZ-derived and two ZB-derived structures are listed for Cu_2ZnGeS_4 as an example. The wurtzite-stannite structure and our new structure have the same primitive cell but differ in the occupation of group-I, -II, and -IV cations, similar to the relation between the ZB-derived kesterite and stannite structures. The WZ structure (hexagonal-close-packed) can be taken as having *ABABAB* packing while the ZB structure (face-centered-cubic) features *ABCABC* packing. The difference between the WZ and ZB structures is a sequential $\frac{\pi}{3}$ rotation of the *C* and above layers. As shown in Fig. 1, the difference between the wurtzite-kesterite structure and the ZB-derived kesterite structure is also a sequential $\frac{\pi}{3}$ rotation of the *C* and above layers. Based on this, we name the new structure wurtzite-kesterite (WKS). Similarly the wurtzite-stannite (WST) structure directly corresponds to the stannite structure.

III. ENERGY STABILITY AND BAND STRUCTURE

A. Calculation methods

The total energy and band structure have been calculated within the density-functional formalism as implemented in the VASP code.[35] For the exchange-correlation potential, we used the generalized gradient approximation (GGA) of Perdew and Wang, known as PW91.[36] The *d* states of group-III and -IV elements are treated explicitly as valence. The interaction between the core electrons and the valence electrons is included by the standard frozen-core projector augmented-wave potentials.[37] An energy cut-off of 300 eV was applied in all cases. For Brillouin-zone integration, we used *k*-point meshes that are equivalent to the $4\times4\times4$ Monkhorst-Pack meshes[38] for an eight-atom cubic unit cell. All lattice vectors and atomic positions were fully relaxed by minimizing the quantum mechanical stresses and forces.

TABLE I. Space groups, lattice constants, and atomic positions of the wurtzite-kesterite, wurtzite-stannite, kesterite, and stannite structured Cu_2ZnGeS_4. The primitive cells of wurtzite-kesterite and wurtzite-stannite structures can be taken as a $2\times2\times1$ supercell of wurtzite structure, and the fractional atomic coordinates correspond to the ideal wurtzite sites before relaxation. For the zinc-blende-derived kesterite and stannite structures, a body-centered tetragonal cell is given here.

Structure	Wurtzite-kesterite	Wurtzite-stannite
Space group	Pc	$Pmn2_1$
Lattice constants (Å)	7.544 6.519 6.226	7.503 6.547 6.226
(0, 0, 0)	Cu	Cu
(1/2, 0, 0)	Zn	Cu
(1/4, 1/2, 0)	Cu	Zn
(3/4, 1/2, 0)	Ge	Ge
(0, 1/3, 1/2)	Zn	Cu
(1/2, 1/3, 1/2)	Cu	Cu
(1/4, 5/6, 1/2)	Ge	Ge
(3/4, 5/6, 1/2)	Cu	Zn
(0, 0, 3/8)	S	S
(1/2, 1/4, 3/8)	S	S
(0, 1/2, 3/8)	S	S
(1/2, 3/4, 3/8)	S	S
(1/3, 0, 7/8)	S	S
(1/3, 0, 7/8)	S	S
(5/6, 1/4, 7/8)	S	S
(5/6, 3/4, 7/8)	S	S

Structure	Kesterite	Stannite
Space group	$I\bar{4}$	$I\bar{4}2m$
Lattice constants (Å)	5.358 5.358 10.641	5.333 5.333 10.741
(0, 0, 0)	Cu	Cu
(1/2, 1/2, 0)	Zn	Cu
(0, 1/2, 1/4)	Cu	Zn
(1/2, 0, 1/4)	Ge	Ge
(0, 0, 1/2)	Zn	Cu
(1/2, 1/2, 1/2)	Cu	Cu
(0, 1/2, 3/4)	Ge	Ge
(1/2, 0, 3/4)	Cu	Zn
(1/4, 1/4, 1/8)	S	S
(3/4, 3/4, 1/8)	S	S
(1/4, 3/4, 3/8)	S	S
(3/4, 1/4, 3/8)	S	S
(1/4, 1/4, 5/8)	S	S
(3/4, 3/4, 5/8)	S	S
(1/4, 3/4, 7/8)	S	S
(3/4, 1/4, 7/8)	S	S

One of the key material electronic parameters is the band gap. While we expect that the trends obtained from a semilocal functional such as PW91 will be reliable, to obtain more quantitative estimations of the band gap changes, we employ a more sophisticated hybrid functional, containing a fixed amount of screened Hartree-Fock nonlocal exchange. In the HSE (Heyd-Scuseria-Ernzerhof) functional,[39] one quarter of exact electron exchange is added to the GGA functional, and a screening of $\omega=0.11$ bohr^{-1} is applied to partition the Coulomb potential into short-range (SR) and long-range (LR) terms. The exchange-correlation functional becomes

$$E_{xc}^{\mathrm{HSE}}(\omega)=E_x^{\mathrm{HSE,SR}}+E_x^{\mathrm{PBE,LR}}+E_c^{\mathrm{PBE}}, \tag{1}$$

where

$$E_x^{\mathrm{HSE,SR}}=\frac{1}{4}E_x^{Fock,\mathrm{SR}}+\frac{3}{4}E_x^{\mathrm{PBE,SR}}. \tag{2}$$

Details of the HSE implementation in VASP are available elsewhere.[40] At this level of theory, the calculated band gaps for CZTS and CZTSe are found to match the experimental values.[8,22,23]

B. Energy stability

After identifying the four ZB- and WZ-derived structures, we will now compare the relative stability between these structures. The calculated total energies for a range of I_2-II-IV-VI_4 compounds are listed in Table II.

From these numbers, we find the following trends: (i) the energy-stability relation between ZB-derived KS and ST is always same as that between WZ-derived WKS and WST, i.e., once KS has lower energy than ST, then WKS has also lower energy than WST, and vice versa. Like the direct relation in the structure, there is corresponding relation in the properties. (ii) Whether for ZB-derived KS and ST or for WZ-derived WKS and WST structures, the KS (WKS) structure is more stable than ST (WST), except for the Cu_2Cd-IV-S_4 series which are more stable in ST (WST) structure. (iii) The energy difference between KS (WKS) and ST (WST) becomes smaller monotonically as the group-IV cations change from Si to Ge to Sn, i.e., the atomic number increases from 14 to 32 to 50. This monotonic decrease is plotted in Fig. 2(a) for ZB-derived KS and ST structures. (iv) The energy difference between the lower-energy ZB-derived and WZ-derived structures, $\Delta E_{\mathrm{WZ\text{-}ZB}}=E_{\mathrm{WZ}}-E_{\mathrm{ZB}}$, increases monotonically as the group-IV cations change from Si to Ge to Sn, also shown in Fig. 2(b). When IV=Si and Ge, Cu_2Cd-IV-S_4, Ag_2Zn-IV-S_4, and Ag_2Cd-IV-S_4 crystallize in the WZ-derived structures as their ground state. (v) All the above trends are common for sulfides and selenides.

From the knowledge about the binary WZ and ZB structures, we know the stability of the WZ-derived structures vs ZB derived is related to the electrostatic Madelung energy. In Table II, we also calculate the Madelung energy for different I_2-II-IV-VI_4 structures, assuming that all atoms are at the ideal lattice sites and in their formal charge states: I^+, II^{2+}, IV^{4+}, and VI^{2-}. The calculated Madelung energy is divided by a factor of 10 to describe the strong electronic screening, and this factor is consistent with the calculated dielectric constant.[23] This simple Madelung model gives energy difference values of the same order as those from first-principles calculations. Among KS, ST, WKS, and WST, WKS has the lowest Madelung energy. Another clear result is that the WZ-derived structure has a lower Madelung energy than the cor-

TABLE II. The total energy (meV/atom) of quaternary semiconductors I_2-II-IV-VI_4 (I=Cu,Ag; II =Zn,Cd; IV=Si,Ge,Sn; VI=S,Se) in different crystal structures relative to that of the kesterite structure. The asterisk indicates the ground-state structure at $T=0$ K. $\Delta E_{WZ\text{-}ZB}$ represents the energy difference between the lowest-energy WZ and ZB structures. The Madelung energy relates to the classical electrostatic energy of different structures.

	Kesterite	Stannite	Wurtzite-kesterite	Wurtzite-stannite	$\Delta E_{WZ\text{-}ZB}$
Cu_2ZnSiS_4	0.0*	4.9	0.3	2.4	0.3
Cu_2ZnGeS_4	0.0*	4.7	3.8	5.6	3.8
Cu_2ZnSnS_4	0.0*	2.8	6.0	7.2	6.0
Cu_2CdSiS_4	0.0	−17.5	−7.8	−19.0*	−1.5
Cu_2CdGeS_4	0.0	−11.9	−3.7	−12.6*	−0.7
Cu_2CdSnS_4	0.0	−3.2*	1.8	−0.6	2.9
Ag_2ZnSiS_4	0.0	30.9	−0.5*	12.5	−0.5
Ag_2ZnGeS_4	0.0	27.5	−0.1*	12.2	−0.1
Ag_2ZnSnS_4	0.0*	18.6	1.2	10.1	0.8
Ag_2CdSiS_4	0.0	10.5	−4.8*	−1.8	−4.8
Ag_2CdGeS_4	0.0	8.6	−3.7*	−0.9	−3.7
Ag_2CdSnS_4	0.0	6.4	−0.9*	1.6	−0.9
$Cu_2ZnSiSe_4$	0.0*	5.6	1.1	3.3	1.1
$Cu_2ZnGeSe_4$	0.0*	4.6	5.6	7.8	5.6
$Cu_2ZnSnSe_4$	0.0*	3.3	8.0	9.6	8.0
$Cu_2CdSiSe_4$	0.0	−15.1	−5.7	−15.3*	−0.2
$Cu_2CdGeSe_4$	0.0	−11.0*	−0.2	−7.8	3.2
$Cu_2CdSnSe_4$	0.0	−2.9*	4.6	2.3	5.2
$Ag_2ZnSiSe_4$	0.0	31.1	−0.4*	12.6	−0.4
$Ag_2ZnGeSe_4$	0.0*	28.3	0.7	14.1	0.7
$Ag_2ZnSnSe_4$	0.0*	19.5	2.8	12.3	2.8
$Ag_2CdSiSe_4$	0.0	10.5	−4.5*	−1.4	−4.5
$Ag_2CdGeSe_4$	0.0	8.4	−2.7*	0.3	−2.7
$Ag_2CdSnSe_4$	0.0*	3.1	1.0	3.5	1.0
Madelung energy	0.0	9.5	−8.8	6.4	−8.8

responding ZB-derived structure, i.e., WKS than KS, and WST than ST, which inherits the character of binary II-VI components. Comparing the Madelung energy with the total energies from first-principles calculations, only Ag_2CdSnS_4 has the same energetic order as the Madelung model, increasing in the order WKS, KS, WST, and ST, and this has two reasons: (i) the Cd-S bond is more ionic than Zn-S bond,[41] so the Madelung-energy contribution to the total energy is large, that is also why CdS crystallizes in the WZ structure as its ground state while ZnS does not. (ii) Ag, Cd, and Sn are in the same row of periodic table, thus their size differences and the strain-energy contribution is small. In other compounds except Ag_2CdSnS_4, the strain energy has significant influence on the relative-energy stability of these structures, thus the total energy depends on the sum of both Madelung and strain energy, which makes different I_2-II-IV-VI_4 compounds have different ground-state structures.

Now we will explain the aforementioned trends according to the Madelung- and strain-energy contributions. For Cu_2Zn-IV-S_4, Ag_2Zn-IV-S_4, and Ag_2Cd-IV-S_4, KS (WKS) has lower strain energy than ST (WST) as well as lower Madelung energy, so either KS or WKS is their ground state, while for Cu_2Cd-IV-S_4, the ST (WST) structure has significantly lower strain energy than KS (WKS), so the total energy is much lower in ST or WST, as shown in Table II. This explanation based on the Madelung and strain energy can also explain the decrease in energy differences as the group-IV cations become larger [see Fig. 2(a)] because the larger size of the group-IV cations and correspondingly larger lattice constant decreases the absolute values of the strain energy and electrostatic Coulomb energy, and thus decreases the total-energy difference.

To show how the size differences between the group-I, -II, and -IV cations influence the strain energy, we also performed a model calculation of the strain energy using the valence force-field method.[42,43] We assume a bond-stretching elastic constant, $\alpha=47$ N/m, and bond-bending elastic constant $\beta=10$ N/m, for all cation-anion bonds and bond angles, respectively. We find that when the I-VI, II-VI, and IV-VI bond lengths are in a certain range the strain energy of the ST structure may be lower than that of the KS structure, although ST is derived from the high strain-energy CuAu structure of ternary I-III-VI_2 compounds.[18] Since assumed

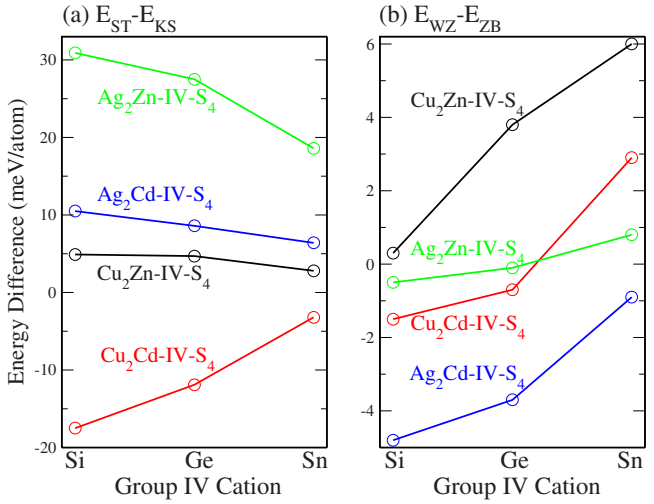

FIG. 2. (Color online) Energy difference change as the group-IV cations change from Si to Ge to Sn: (a) energy difference between the ST and KS structures, (b) energy difference between the WZ- and ZB-derived structures with lower energy.

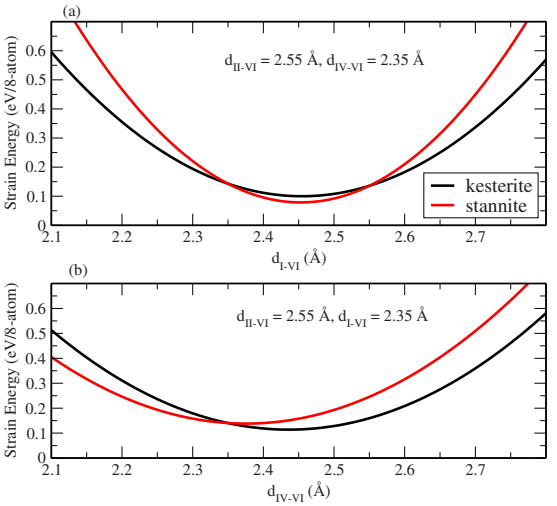

FIG. 3. (Color online) The strain-energy change in kesterite and stannite structures as a function of the I-VI, II-VI, and IV-VI bond length. The strain energy is calculated using the valence force field method, and α=47 N/m, β=10 N/m for all cation-anion bonds and bond angles.

parameters are used for α and β, the values cannot be directly compared with first-principles total-energy calculations, but the trend is consistent, e.g., when the I-VI bond length is shorter than II-VI and longer than IV-VI, like Cu-S compared to Cd-S and Ge-S, the strain energy of ST structure becomes lower than that of KS [Fig. 3(b)], which agrees with the results for Cu_2CdGeS_4 and Cu_2CdSiS_4 shown in Table II. The first-principles calculations further confirm the strain-energy influence: we found that the energy of the KS structure is always lower than the ST structure if all the bond lengths are fixed to be the same, but when the bond lengths are allowed to relax to their equilibrium values, the energy stability will be inverted for Cu_2CdGeS_4 and Cu_2CdSiS_4.

For the relative stability between the ZB-derived and WZ-derived structures, the Madelung energy plays the dominant role. Ag-S and Cd-S bonds have stronger ionicity than Cu-S and Zn-S bonds,[41] so Cu_2Cd-IV-S_4, Ag_2Zn-IV-S_4, and Ag_2Cd-IV-S_4 with IV=Si and Ge, crystallize in WZ-derived structures as their ground state, however, when group-IV cations become larger, the Madelung-energy priority of WZ-derived structures will be smaller, then the ZB-derived structures become the ground state, e.g., for Cu_2CdSnS_4 and Ag_2ZnSnS_4. This explanation is consistent with the monotonic increase in the energy difference $\Delta E_{WZ\text{-}ZB}=E_{WZ}-E_{ZB}$ as the group-IV cations become larger, shown in Fig. 2(b).

Our discussion has so far concentrated on the results for sulfides, but for selenides we find that all the trends are similar, despite the weaker ionicity and larger size of selenides makes the values different. The weaker ionicity makes the contribution from Madelung energy smaller, and thus smaller possibility for WZ-derived structures being the ground state, e.g., the ground state of Ag_2CdSnS_4 is WKS, while that of $Ag_2CdSnSe_4$ is KS.

Generally speaking, we find that the I_2-II-IV-VI_4 compounds prefer the WZ-derived structures when there are strong ionic cations such as Cd and Ag, but the relative energy priority of WZ-derived structures become weaker when the group-IV cations and group-VI anions become larger. This trend explains the experimental observation that many Sn-containing compounds crystallize preferably in a sphalerite superstructure (ZB-derived) while the silicon-containing compounds crystallize in a wurtzite superstructure (WZ-derived) types.[20,29,44] For Cu_2ZnGeS_4, Doverspike *et al.* found that a low-temperature modification crystallizes in the ST structure and the transformation to the WST structure takes place at 1083 K,[28] i.e., the WZ-derived structure is the high-temperature modification, like WZ is the high-temperature modification of ZnS. A similar high-temperature WZ-derived phase is also observed by Tsuji *et al.*[10] This observation is consistent with our calculation because the WKS structure is 3.8 meV/atom higher in energy than the KS structure, and this energy difference can be overcome at high temperature.

It should be noted that in the structure determination of Cu_2ZnGeS_4 and $Cu_2ZnGeSe_4$ through the refinement of x-ray diffraction data, usually the ST structure is attributed to the ZB-derived structure and WST structure to the WZ-derived structure,[28,45] which is, in fact, a confusion. Because Cu, Zn, and Ge have close atomic number and thus similar form factor, different occupations of these cations, i.e., different structure configurations such as KS and ST, give similar x-ray diffraction pattern, therefore previous experiments usually take KS for ST, and take WKS for WST, while our first-principles calculation shows clearly that KS and WKS structures should be more stable than ST and WST structures. Another reason for the easy confusion is that Cu and Zn cations are partially disordered in the Cu+Zn planes of KS structure, which makes the KS structure exhibit the same symmetry as ST and be confused with ST. This partial occupational disorder in KS Cu_2ZnSnS_4 has been observed by neutron-scattering experiments.[21] For WZ-derived WKS structure, we find that the Cu and Zn partial disorder are also very easy to form and change the symmetry of WKS to the

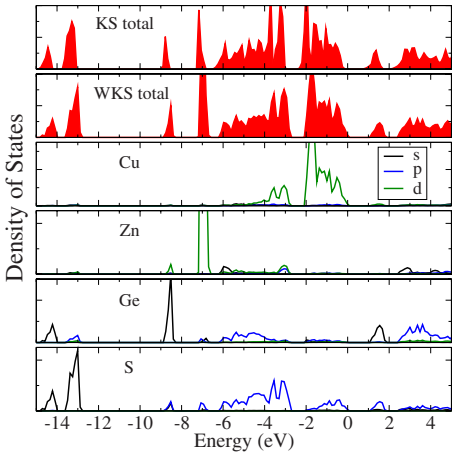

FIG. 4. (Color online) Total and partial electronic density of states of KS and WKS Cu_2ZnGeS_4. The top of the valence band is set to 0 eV.

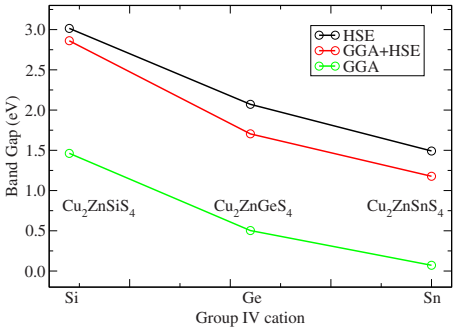

FIG. 5. (Color online) Calculated band gap of kesterite Cu_2Zn-IV-S_4 which decreases as the group-IV cations change from Si to Ge to Sn. The gap is calculated using three different methods: (i) GGA: the electronic and atomic structures are relaxed using the GGA functional, (ii) GGA+HSE: a static HSE electronic structure calculation for the crystal structure relaxed using the GGA, (iii) HSE: the electronic and atomic structures are relaxed using the HSE functional.

same as WST. As shown in Fig. 1(a), there are two Cu+Zn planes parallel to the paper surface. If the two planes in one unit cell are shifted together by half a basis vector along Cu→Zn→Cu axis, while the same planes in other unit cells are fixed, the new structure still satisfies the octet rule, i.e., the energy cost is small, and according to our calculation, the energy cost is only 0.1 meV/atom for Cu_2ZnGeS_4 and almost zero for Cu_2ZnSnS_4, indicating that the shift can happen easily and randomly, which results in the partial disorder.

The structural complexity found in these materials suggests that it will be necessary not only to use conventional x-ray diffraction but also to apply more advanced experimental techniques, such as neutron scattering and inelastic or resonant x-ray scattering[21] to distinguish between various structure models. For example, previously only the WST structure was considered in fitting the x-ray diffraction pattern of Cu_2ZnSiS_4, Cu_2ZnGeS_4, and Ag_2CdGeS_4.[20,28,45] However, our calculations show that for these compounds, the WKS structure will also fit the pattern, and the calculated lattice constants of the WKS structures agree well with the experimental values, e.g., for Cu_2ZnSiS_4, the measured values are 7.435 Å, 6.396 Å, and 6.135 Å for *a*, *b*, and *c*, respectively, and our calculated results are 7.544, 6.519, and 6.226 Å. The slight overestimation is common at the GGA-DFT level of theory. The calculated total energies are also lower in the WKS structure than in the WST for these compounds. Experimental testing of our predicted structures for these compounds is called for.

C. Band structure

For the electronic band structure of quaternary I_2-II-IV-VI_4 semiconductors, since in WZ-derived and ZB-derived structures the anions are both tetrahedrally coordinated by cations (i.e., the bonding character is similar), the band components are also similar, as shown clearly by the calculated density of states in Fig. 4. From the calculation, the following results can be found: (i) I_2-II-IV-VI_4 semiconductors have usually direct band gaps at the Γ point, (ii) the top valence band is mainly the antibonding component of the *p-d* hybridization between the group-VI anion and group-I cation, as shown in Fig. 4, (iii) the bottom conduction band is mainly the antibonding component of the *s-s* and *s-p* hybridization between the group-IV cation and group-VI anion,[18] except for those containing Si, the group-I and -II cations also have significant contribution to the bottom conduction band as well as Si and group-VI anion.

One consequence of the aforementioned band component is that as the group-IV cations change from Si to Ge and then to Sn, the band gap decreases in order, as shown in Fig. 5. This is due to the increasing size of Si, Ge, and Sn weakens the *s-s* and *s-p* level repulsion between IV and VI, making the antibonding conduction-band minimum decrease from Cu_2ZnSiS_4 to Cu_2ZnGeS_4 to Cu_2ZnSnS_4. Since GGA usually underestimates the band gap significantly, we also calculate the band gaps using a hybrid density functional. As shown in Fig. 5, the HSE functional opens up the GGA band gap significantly, but the trend is nearly unchanged. According to these results, we find that the gap enhancement by HSE includes two contributions: (i) when we calculate the band gap using HSE for the crystal structure optimized using GGA, the band gap is enlarged by about 1.3 eV relative to the GGA value, (ii) when we relax the lattice constants and internal atomic positions for the crystal structure using HSE, the gap will be further enlarged by about 0.2 eV. Although there are significant band-gap enhancements, the relative gap differences are conserved for the three different methods, indicating that GGA gives correct band-gap differences for Cu_2Zn-IV-S_4, and the band gap decrease as the group-IV cations become larger is reliable.

Comparing the band gaps of different structures, we find an obvious trend: the gap decreases in the order WKS, KS, WST, and ST, as shown in Fig. 6 for Cu_2Zn-IV-S_4. In other words, the band gap of ZB-derived structure is always smaller than the corresponding WZ-derived structure, i.e., KS smaller than WKS and ST smaller than WST. The same trend also exists for binary zinc-blende and wurtzite semiconductors, which has been explained by Wei and Zhang.[46] They showed that at the Γ point, the electronic states of the

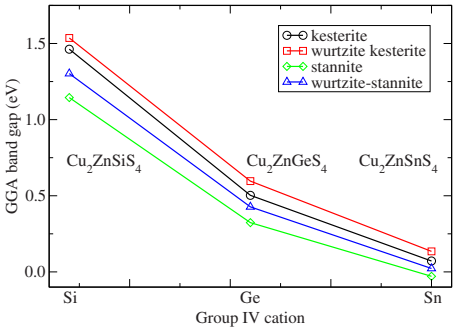

FIG. 6. (Color online) GGA calculated band gap of Cu_2Zn-IV-S_4 which decreases as the group-IV cations change from Si to Ge to Sn.

WZ structure can be derived directly from those of ZB structure, and the conduction-band minimum states are both Γ_1 states, but due to the lower symmetry of the WZ structure, the valence-band maximum states of WZ are Γ_1 and Γ_6, derived from the ZB Γ_{15} state. Therefore in the WZ structure the two Γ_1 states at the conduction and valence bands will interact with and repel each other, which will increase the band gap, but in the ZB structure the Γ_1 and Γ_{15} states do not interact. This explanation works also for the quaternary semiconductors, where the interaction still exists for the WZ-derived structures and does not exist for the ZB-derived structures because although the valence-band maximum Γ_{15} state splits into Γ_4 and Γ_5,[47] they do not interact with Γ_1 due to the different wave-function symmetries.

IV. CONCLUSION

We report the crystal structures of two wurtzite analogs to the zinc-blende-derived kesterite and stannite structures for quaternary chalcogenide semiconductors. The wurtzite-kesterite structure has been ignored in the previous structural characterization of I_2-II-IV-VI_4 semiconductors. The energy stability of different structures is studied according to the strain- and Coulomb-energy contributions, showing a dependence on the size and ionicity of the component atoms. Generally speaking, quaternary semiconductors with small and strongly ionic elements prefer the wurtzite-kesterite or wurtzite-stannite structures. The band structure of wurtzite-derived structures are similar to those of zinc-blende-derived structures, but the band gaps are relatively larger. Experimental validation of our predicted structures is called for.

ACKNOWLEDGMENTS

The work in Fudan is supported by the Natural Sciences Foundation (NSF) of China (Grants No. 10934002 and No. 1095011032), the Research Program of Shanghai municipality and MOE, the Special Funds for Major State Basic Research. The work in ECNU is supported by NSF of Shanghai (Grant No. 10ZR1408800) and NSF of China (Grant No. 60990312) and the Fundamental Research Funds for the Central Universities. A.W. would like to acknowledge funding from NSF of China (Grant No. 10950110324). The work at NREL is funded by the U.S. Department of Energy under Contract No. DE-AC36-08GO28308.

[1] H. Katagiri, K. Jimbo, W. S. Maw, K. Oishi, M. Yamazaki, H. Araki, and A. Takeuchi, Thin Solid Films **517**, 2455 (2009).
[2] K. Tanaka, M. Oonuki, N. Moritake, and H. Uchiki, Sol. Energy Mater. Sol. Cells **93**, 583 (2009).
[3] A. Weber, S. Schmidt, D. Abou-Ras, P. Schubert-Bischoff, I. Denks, R. Mainz, and H. W. Schock, Appl. Phys. Lett. **95**, 041904 (2009).
[4] Q. Guo, H. W. Hillhouse, and R. Agrawal, J. Am. Chem. Soc. **131**, 11672 (2009).
[5] C. Steinhagen, M. G. Panthani, V. Akhavan, B. Goodfellow, B. Koo, and B. A. Korgel, J. Am. Chem. Soc. **131**, 12554 (2009).
[6] J. Scragg, P. Dale, and L. Peter, Thin Solid Films **517**, 2481 (2009).
[7] A. Shavel, J. Arbiol, and A. Cabot, J. Am. Chem. Soc. **132**, 4514 (2010).
[8] S. Ahn, S. Jung, J. Gwak, A. Cho, K. Shin, K. Yoon, D. Park, H. Cheong, and J. H. Yun, Appl. Phys. Lett. **97**, 021905 (2010).
[9] T. K. Todorov, K. B. Reuter, and D. B. Mitzi, Adv. Mater. **22**, E156 (2010).
[10] I. Tsuji, Y. Shimodaira, H. Kato, H. Kobayashi, and A. Kudo, Chem. Mater. **22**, 1402 (2010).
[11] X. Y. Shi, F. Q. Huang, M. L. Liu, and L. D. Chen, Appl. Phys. Lett. **94**, 122103 (2009).
[12] M.-L. Liu, I.-W. Chen, F.-Q. Huang, and L.-D. Chen, Adv. Mater. **21**, 3808 (2009).
[13] C. Sevik and T. Çağin, Appl. Phys. Lett. **95**, 112105 (2009).
[14] C. Sevik and T. Cagin, Phys. Rev. B **82**, 045202 (2010).
[15] T. Fries, Y. Shapira, F. Palacio, M. C. Morón, G. J. McIntyre, R. Kershaw, A. Wold, and E. J. McNiff, Phys. Rev. B **56**, 5424 (1997).
[16] V. P. Sachanyuk, I. D. Olekseyuk, and O. V. Parasyuk, Phys. Status Solidi A **203**, 459 (2006).
[17] G. Nénert and T. T. M. Palstra, J. Phys.: Condens. Matter **21**, 176002 (2009).
[18] S. Chen, X. G. Gong, A. Walsh, and S.-H. Wei, Phys. Rev. B **79**, 165211 (2009).
[19] V. Petrykin, K. Tomita, M. Kakihana, Y. Shimodaira, A. Kudo, H. Sawa, and T. Kakiuchi, Photon Factory Act. Rep. **23**, Part B (2006).
[20] M. Bohm, G. Huber, A. MacKinnon, O. Madelung, A. Scharmann, and E.-G. Scharmer, *Physics of Ternary Compounds* (Springer, New York, 1985).
[21] S. Schorr, H. J. Hoebler, and M. Tovar, Eur. J. Mineral. **19**, 65 (2007).
[22] S. Chen, X. G. Gong, A. Walsh, and S.-H. Wei, Appl. Phys. Lett. **94**, 041903 (2009).
[23] J. Paier, R. Asahi, A. Nagoya, and G. Kresse, Phys. Rev. B **79**, 115126 (2009).
[24] G. N. Lewis, J. Am. Chem. Soc. **38**, 762 (1916).
[25] L. Pauling, J. Am. Chem. Soc. **51**, 1010 (1929).

[26] B. Koo, R. N. Patel, and B. A. Korgel, Chem. Mater. **21**, 1962 (2009).
[27] M. E. Norako and R. L. Brutchey, Chem. Mater. **22**, 1613 (2010).
[28] K. Doverspike, K. Dwight, and A. Wold, Chem. Mater. **2**, 194 (1990).
[29] T. Bernert, M. Zabel, and A. Pfitzner, J. Solid State Chem. **179**, 849 (2006).
[30] Y. Luo, S. Chen, X. G. Gong, and S.-H. Wei (unpublished).
[31] S.-H. Wei, S. B. Zhang, and A. Zunger, Phys. Rev. B **59**, R2478 (1999).
[32] X. L. Chen, A.-M. Lamarche, G. Lamarche, and J. C. Woolley, J. Phys.: Condens. Matter **5**, 7143 (1993).
[33] W. H. Baur and T. J. McLarnan, J. Solid State Chem. **42**, 300 (1982).
[34] T. J. McLarnan and W. H. Baur, J. Solid State Chem. **42**, 283 (1982).
[35] G. Kresse and J. Furthmuller, Phys. Rev. B **54**, 11169 (1996).
[36] J. P. Perdew, J. A. Chevary, S. H. Vosko, K. A. Jackson, M. R. Pederson, D. J. Singh, and C. Fiolhais, Phys. Rev. B **46**, 6671 (1992).
[37] G. Kresse and D. Joubert, Phys. Rev. B **59**, 1758 (1999).
[38] H. J. Monkhorst and J. D. Pack, Phys. Rev. B **13**, 5188 (1976).
[39] J. Heyd, G. E. Scuseria, and M. Ernzerhof, J. Chem. Phys. **118**, 8207 (2003).
[40] J. Paier, M. Marsman, K. Hummer, G. Kresse, I. C. Gerber, and J. G. Ángyán, J. Chem. Phys. **124**, 154709 (2006).
[41] J. C. Phillips, *Bonds and Bands in Semiconductors* (Academic Press, New York, 1973).
[42] P. Keating, Phys. Rev. **145**, 637 (1966).
[43] J. L. Martins and A. Zunger, Phys. Rev. B **30**, 6217 (1984).
[44] W. Schäfer and R. Nitsche, Z. Kristallogr. **145**, 356 (1977).
[45] O. V. Parasyuk, L. V. Piskach, Y. E. Romanyuk, I. D. Olekseyuk, V. I. Zaremba, and V. I. Pekhnyo, J. Alloys Compd. **397**, 85 (2005).
[46] S.-H. Wei and S. B. Zhang, Phys. Rev. B **62**, 6944 (2000).
[47] S. Chen, X. G. Gong, and S.-H. Wei, Phys. Rev. B **75**, 205209 (2007).